2002-2003 Report

SAFL Consortium

XES R02-1

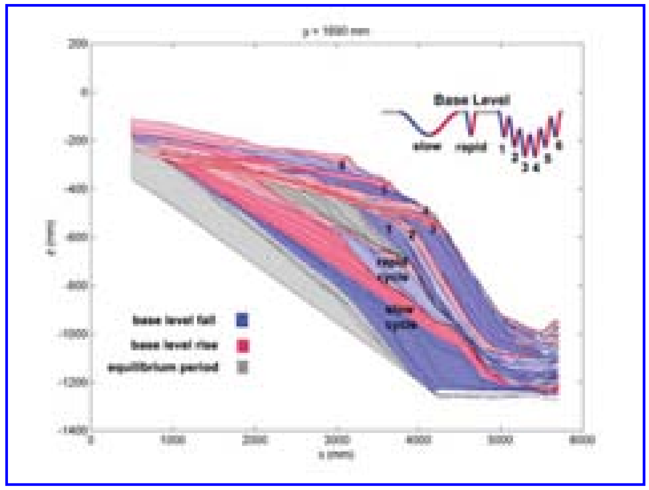

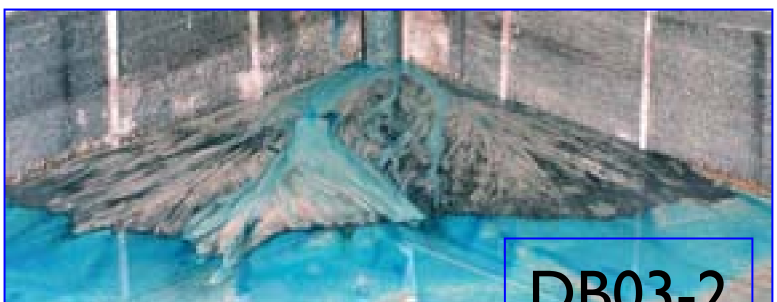

DB03-2

XES R01-1

DB03-1

2002-2003 Report
SAFL Consortium

Table of Contents

2002-2003 SAFL Industrial Consortium Report

Delta Basin Run 03-1 Report: High Resolution Stratigraphy

High-Resolution Stratigraphy: Delta Basin 03-1

Ben Sheets, Michael Kelberer

Summary

One of our main accomplishments during the past year was the establishment of the delta basin as a viable alternate experimental facility to the XES basin. Given the complexities and time necessary for full-scale XES runs, we find the delta basin to be a more simple and quick arrangement with which to conduct experiments where complex subsidence geometries are not needed, but base level control, topographic measurements, and detailed digital records are essential. Two research experiments were conducted in the delta basin this year. The first, motivated by results from the 99-1 XES alluvial architecture experiment, is the subject of this report. The latter is discussed elsewhere in this volume (DB 03-2: Low Froude Number Experiment)

The first delta basin experiment (DB 03-1) was motivated by the fact that the four-hour spacing of the topographic scans during the XES 99-1 experiment was too infrequent to capture individual depositional events, such as individual channel-filling episodes or overbank splays. The objective, therefore, was to form a deposit comparable in character to the deposit of the 99-1 experiment, but to do so while taking topographic measurements at two-minute intervals—some 900 total measurements.

Examination of these data is ongoing, but preliminary analysis has highlighted several characteristics of the experimental alluvial deposition. First, the concave-up 'channel' structures we identify in our deposits are, indeed, formed by the pervasive confluence scours that occur in the experimental fluvial systems, though their filling may occur substantially later. The channel structures are, therefore, comparable in scale and aspect ratio to the surface scours. Second, the filling of these structures is rapid, though not necessarily continuous. Third, net aggradation in these systems is accomplished through a shifting and quasi-random patchwork of depositional events, most of which are short-lived. And fourth, despite this quasi-random behavior, there is some order to the depositional packages produced in short-term aggradational events—their aspect ratios approximate those of the fluvial channels and 'fans.'

Introduction

One of the most interesting, and most confounding, aspects of the first experiment in the Jurassic Tank facility was the obvious relationship between the fluvial morphology of the experimental system and the deposits it created. Interesting, because of the bimodal nature of the stratigraphy—both high aspect ratio sheet deposits and low aspect ratio channel (or ribbon) deposits were created. Further, there was wide variability in the character of the channel fill, which ranged from exclusively sand to exclusively coal—features presumably related to the flows responsible for their deposition.

Confounding, because the relationship between flow morphology and stratigraphy was difficult to evaluate. The 8 mm video documentation of the surface from the XES 99-1 experiment is not detailed enough to properly measure, and spatially locate, individual flow events. Further, the high-resolution still images, which were taken at ten-minute intervals, are too infrequent to capture short-lived flow processes.

Despite this, we were able to assemble a crude understanding of how flow processes led to particular stratigraphic features. In particular, there was a clear relationship between erosively-based channel structures and fluvial confluence-scours, as well as between depositional sheets and overbank sheetflows. This work is detailed in Cazanacli *et al.* (2002), and Sheets *et al.* (2002).

The motivation for the present experiment, then, was to create stratigraphy of a comparable character to XES 99-1, but to carefully record both the topography and surface morphology with sufficient temporal resolution to observe and quantify the deposition of individual channel fills and sheets. We used sediment and water discharge rates comparable to XES 99-1, and as the subsidence pattern has little influence on deposition on short time-scales, we decided that the simple piston-style geometry possible in the delta basin was appropriate.

The data obtained from run DB 03-1 will be used primarily to investigate the relationship between surface morphology and stratigraphy, and to determine quantitatively what events produce the stratigraphic record. The frequent topographic scans, in combination with records of the fluvial surface allow us to compare general morphological statistics—flow occupation, depth, or width—with short-term aggradation rates.

Experiment	Q_w (Ls^{-1})	Q_s (Ls^{-1})	Q_w:Q_s	Avg. Aggradation rate (mm/hr)	Avg. Slope
DB 03-1	0.4	0.01	40:1	5.0	0.05
XES 99-1 (stage 2)	0.53	0.0136	39:1	7.0	0.047

Table 1: Comparison of experimental parameters between DB03-1 and JT99-1

The Experiment

In order to create stratigraphy comparable to that of XES experiment 99-1, the experimental parameters in DB 03-1 were modeled on Stage 2 of the 99-1 experiment (see Table 1). Subsidence in the delta basin is simulated via a gradual rise in the base level, at a rate equal to the total sediment discharge (Q_s) divided by the desired fluvial system area. This reproduces a simple-piston subsidence geometry.

The delta basin is 5 m by 5 m (25 m^2) and 0.61 m deep (See Figure 1). Sediment and water were mixed in a funnel and fed into the basin at one corner. This produced an approximately radially symmetrical fluvial system, which averaged 2.50 m from source to shoreline. The edges of the basin were artificially rough-

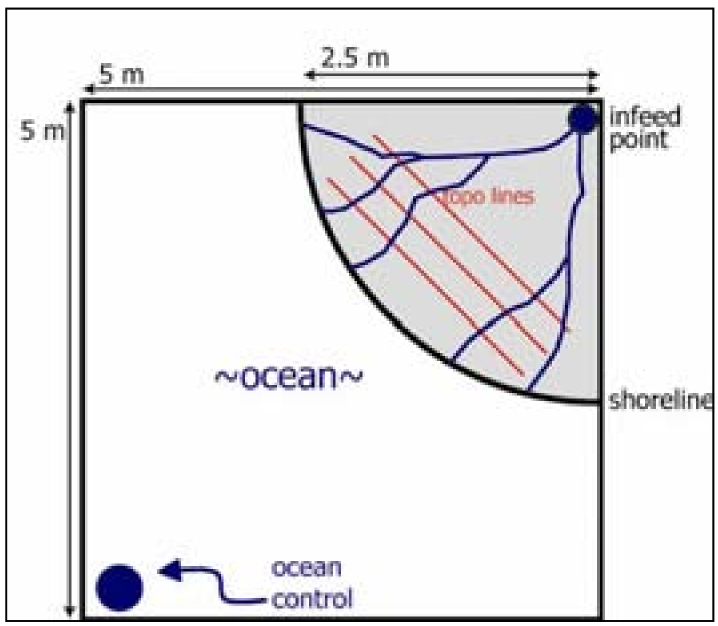

Figure 1: plan-view sketch of the delta basin and experimental set-up for DB 03-1

ened, in order to direct the channels away from the walls. The eustatic base level was maintained through a variable-discharge siphon located in the opposite corner of the basin. Though we imposed a gradual base-level rise, in order to simulate subsidence, the shoreline maintained an approximately constant downstream position through the experiment, because the sediment feed was matched to the eustatic rise rate.

The sediment mixture in the DB 03-1 experiment contrasted slightly with that of XES 99-1. We used a mixture comprising 70% 120 □m silica sand and 30% bimodal (190 and 460 mm) anthracite coal (the proportions were 60% and 40%, respectively, in XES 99-1). We employed this mixture to enhance the stability of the deposit, in order to make sectioning easier.

The morphology of the fluvial system was recorded with two cameras, a standard VHS, which served as a time-lapse video log of the experiment, and a Nikon D-100, which recorded a high-resolution image of the surface at 15 s intervals. The latter camera provided the primary record that we use for analysis of flow morphology.

Topographic measurements were taken in a manner modeled on the XES subaerial laser topography scanner. In contrast to XES, however, where the topography of the entire fluvial surface is recorded periodically, we chose to monitor the topography at 2 minute intervals along three flow-perpendicular transects, located 1.50 m, 1.75 m, and 2.00 m from the infeed point (Figure 1). This arrangement allowed instantaneous (the exposure time of the camera) measurements, rather than the 30 to 45 minutes required for a full-surface scan. With this system, we obtained measurements with a resolution of approximately 0.8 mm.

The DB 03-1 experiment was run for 30 hours, and produced an average of 20 cm of stratigraphy. We sectioned, peeled, and imaged the deposit at each of the topographic strike-transects, and created a composite dip-section along the streamwise centerline of the deposit.

Data Analysis

As the focus of this experiment was to record the construction of alluvial stratigraphy with very high temporal resolution, we concentrated our analysis of both the fluvial processes and the deposit at the three topographic transects. The first step in the analysis was to correct and extract the topographic data from the experiment. The camera that took the topographic image was arranged such that it could also be used to image the strike-sections. By applying the same corrections for radial and perspective distortions to both sets of images, we have been able to overlay the topographic scan lines on the stratigraphy. Images of the surface morphology (some 7200) were also corrected to be accurate at the topographic transects. We have made digital time-lapse movies of much of the experiment, though they appear distorted in plan view due to these corrections.

The topographic images were further processed in order to make quantitative measurements of aggradation rates. Figures in this document appear both with pixel units and mm units, as there is a linear relationship between the two, though we have not yet applied this correction to all of the data.

To date, we have approached this topographic data in several ways. In addition to aggradation and erosion rates, we have measured the size and aspect ratio of depositional packages over time intervals from 2 to 20 minutes. Further, we have considered the timing of aggradational and erosional intervals at specific points and over wider sections of the topographic transects.

Evolution of surface topography

As we have learned from previous experiments, relatively high ratios of water to sediment (40:1) in the infeed lead to steep slopes, and near-critical flows. The fluvial surface during DB 03-1 was no exception. As in XES 99-1, the most noticeable morphological features in records of the fluvial surface are the erosional confluence scours. These features tend to migrate upstream with time, and dissipate near the infeed point, similar to those documented in XES 99-1 (Cazanacli et al., 2002; Sheets et al., 2002). Associated with these scours are downstream flow expansions, which, due to decreasing velocities, are clearly depositional. In the XES 99-1 experiment and its deposits, these two morphological features seem reflected in the stratigraphy. Indeed, the similarity in aspect ratios between scours and ribbon channel bodies, as well as flow expansions and sheet sands, provide an intuitive link between surface and deposit. The data from this experiment (DB 03-1), however, allows us to monitor the topographic evolution of these surface morphological features, in order to more aptly relate them to their deposits. To this end, we have assembled an initial statistical picture of short-term aggradation through the experiment.

Aggradation on two-minute intervals is remarkably discontinuous—both temporally and spatially. Figure 2 shows aggradation averaged across the entire width of each topographic transect, and

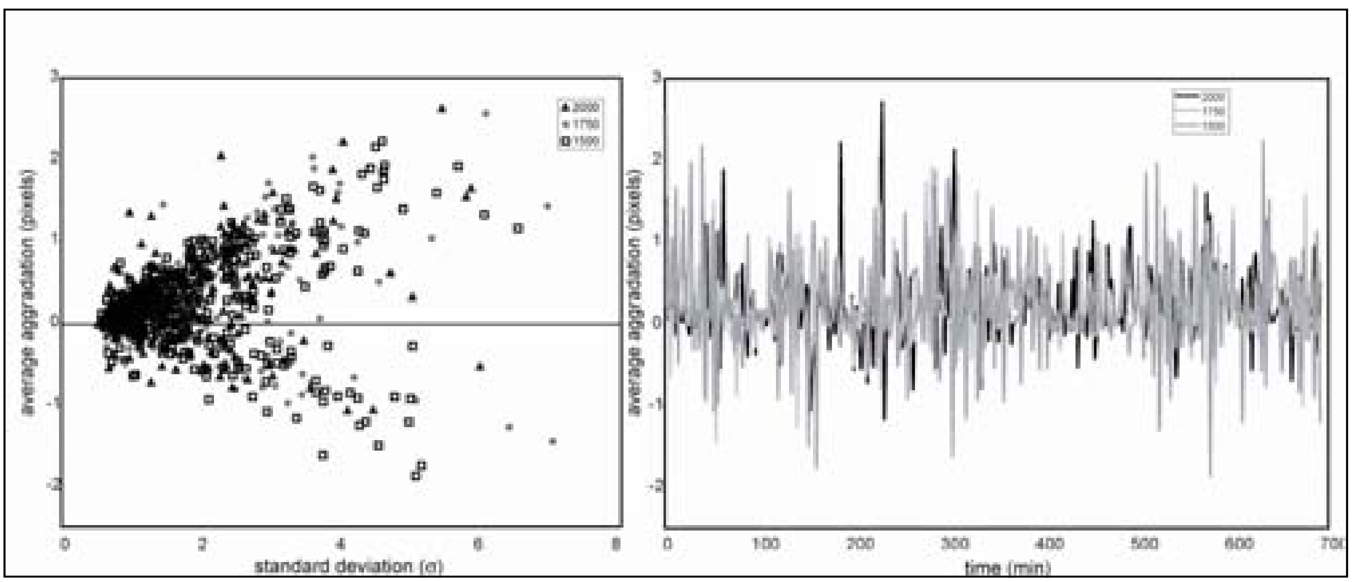

Figure 2: Left: plot of average aggradation along each topographic transect versus the standard deviation of aggradation over the same time interval. **Right**: average aggradation along each topographic transect versus time before the end of the experiment (0 = end of experiment).

illustrates both temporal and spatial variability in topography through the last ten hours of the experiment. When spatially averaged in this way the behavior seems quasi-random, with standard deviation proportional to average aggradation. While the long-term aggradation rate is necessarily the externally-imposed subsidence rate, on short time-intervals this external signal is obscured.

On the other end of the spectrum, when episodes of deposition and erosion are measured at a point (rather than along an entire transect), more order emerges. At each of nine points (three per transect) successive elevations are differenced, and the net change compared with a chosen threshold. When this threshold is exceeded, the vertical size and time of the 'event' recorded. Table 2 shows data

		Erosion Events					Deposition Events					
Threshold	topo line	#/hour	mm/hour	total events	total erosion		#/hour	mm/hour	total events	total deposition		Erosion/Deposition
4mm	**1.50**	10.4	-7.2	300	-207		21.0	13.4	607	386		54%
	1.75	11.9	-9.1	344	-262		19.2	14.0	555	403		65%
	2.00	15.6	-12.5	451	-360		25.6	18.0	738	518		70%
3mm	**1.50**	14.1	-8.4	406	-242		30	16	878	476		51%
	1.75	17.3	-11.0	499	-318		36	19	1028	562		57%
	2.00	18.8	-13.9	542	-400		29	20	851	569		70%
2mm	**1.50**	17.3	-9.2	500	-266		48.8	21.1	1409	608		44%
	1.75	20.1	-11.9	579	-343		51.3	23.5	1480	678		51%
	2.00	29.6	-17.0	855	-490		61.2	27.9	1768	805		61%

Table 2: Statistics for erosion and deposition events captured at differing depth thresholds

obtained using various thresholds through the entire experiment. As the data collected with a 3mm value most closely resembles the actual deposit thickness, it would seem that the smaller thresholds capture too much noise, and the larger thresholds too little deposition.

There is a weak relationship between the size (mm) of these events and the interval of time that had passed since the preceding event of that type (see Figure 3). This suggests, as expected, that the system was sediment dominated—the entire surface was well supplied. Even the longest depositional hiatuses in this system did not create substantial differential topography. Had they done so, the thickness of aggradational events would presumably be related to hiatus length, as the system struggled to fill holes.

The magnitude, expressed as a depth, of depositional events is significantly (15%) smaller, on average, than the magnitude of erosion events. Depositional events, however, occur approximately twice as often (see Table 3). The sum total erosion is consistently—across event sizes and locations—about 60% of the sum total ag-

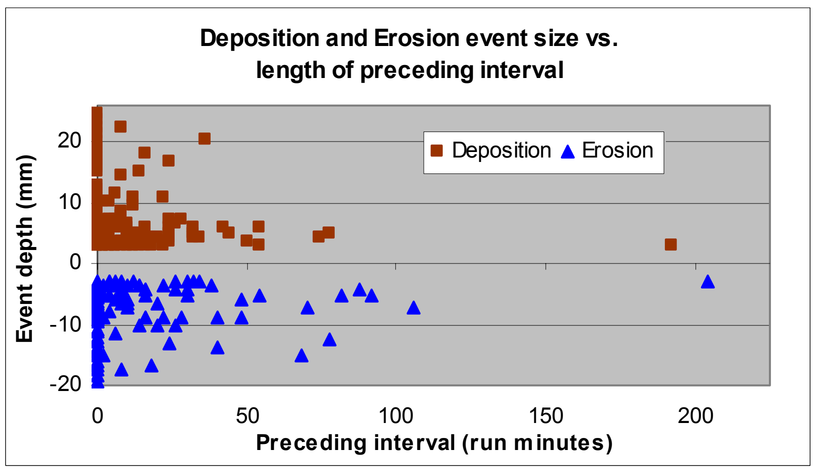

Figure 3: Erosion and deposition events versus the length of

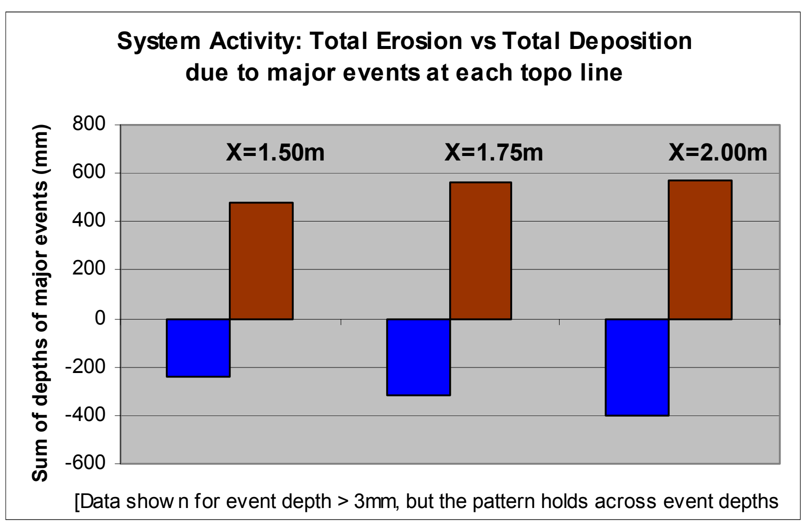

Figure 4: System activity—total erosion and deposition by events larger than 3 mm at each topographic transect.

gradation (see Figure 4). This system took three steps backwards for every five forward.

The frequency distribution of depositional and erosional events indicates a distinct preference, in both cases, for events approximately 6 mm deep (see Figure 5). The time-average tendency for erosional events to have larger magnitudes is reflected in figure 5 by the relatively large number of erosional events up to 10 mm in depth. It seems that erosion, largely the product of the confluence scours discussed above, may range up to 10 mm in size, whereas subsequent aggradation frequently does not. This may be due to the tendency for aggradation to occur in relatively thin sheets, whereas erosion is typically the product of confluence and scour.

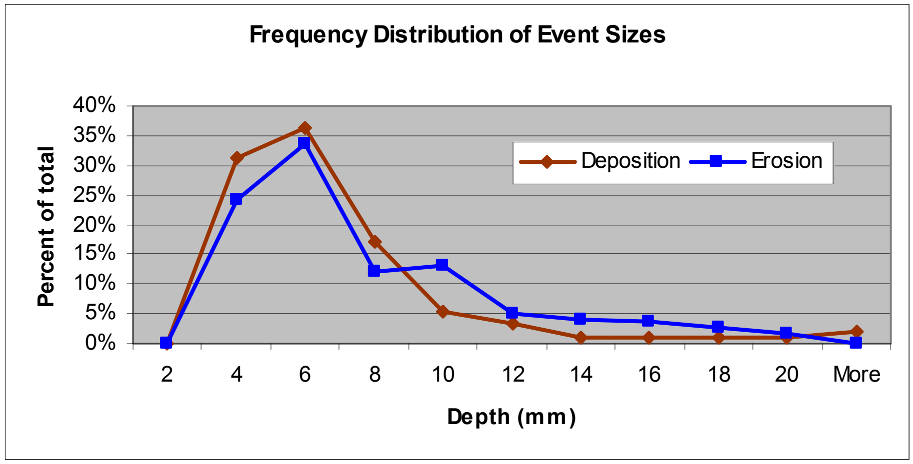

Figure 5: Frequency distribution of event depths

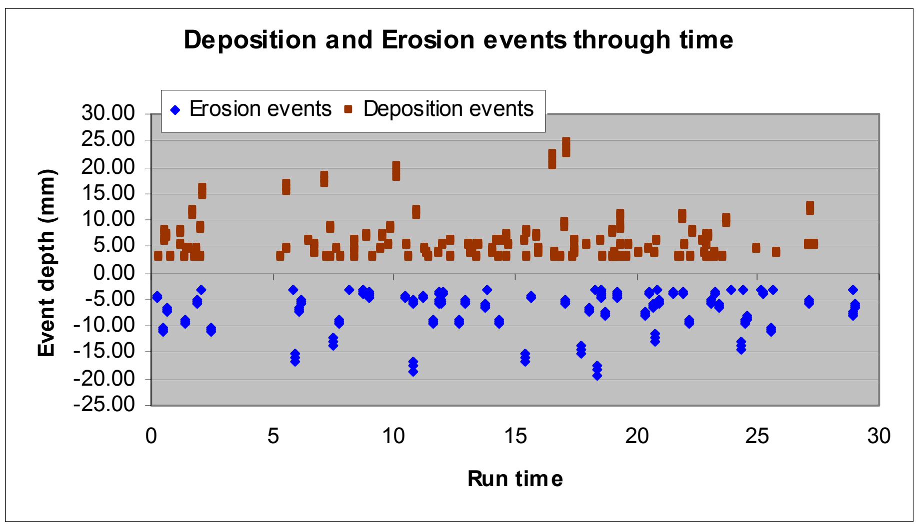

Figure 6: Erosional and depositional event depths through the experiment

Further, the mean depth and spacing of these events (erosion and deposition) are approximately constant through the experiment (see Figure 6). This is presumably due to constant external forcing. At this point, the DB 03-1 experiment provides only one data point with respect to many of these statistics. As the mechanism now exists to take these topography measurements for all delta basin experiments, in particular the low Froude number experiment, by comparing these measurements across runs, we can improve our understanding of the relationship between topographic evolution and external forcing.

The shape of deposition

Somewhere between the whole-transect and individual point topographic statistics discussed above lies the actual shape of depositional packages. In order to quantify such shapes, we measured the cross-sectional areas and aspect ratios of discrete depositional packages over 2, 4, 6, 8, 10, and 20 minute intervals. A depositional package is defined as a contiguous two-dimensional depositional body that is bounded on both ends by zero aggradation (see Figure 7 on next page).

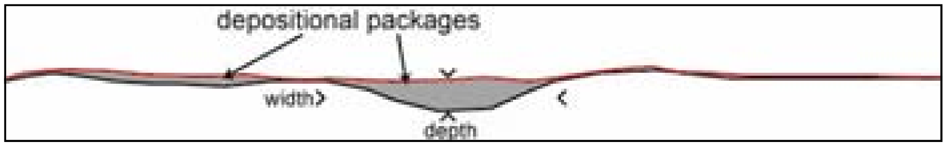

Figure 7: sketch of depositional package definition. Black and red lines represent topography at beginning and end of time interval, respectively. Depositional packages shaded gray. Note that the definition of depth used here is the maximum

The shape of the depositional packages, as measured here, is highly variable, though there is some order. There is a relatively sharp upper limit to the measured aspect ratios (see Figure 8a,b). Figure 8a illustrates this, as for increasing widths, the minimum depth increases. Further, Figure 8b shows that this upper limit is sharper for relatively small depositional packages. This phenomenon is presumably related to a physical upper aspect limit for the surface flows themselves. Given a certain amount of water in a channel, which itself limits the size of an instantaneous depositional package, there is a maximum width that the channel may attain—so limiting the aspect of any resultant deposit. As larger flows

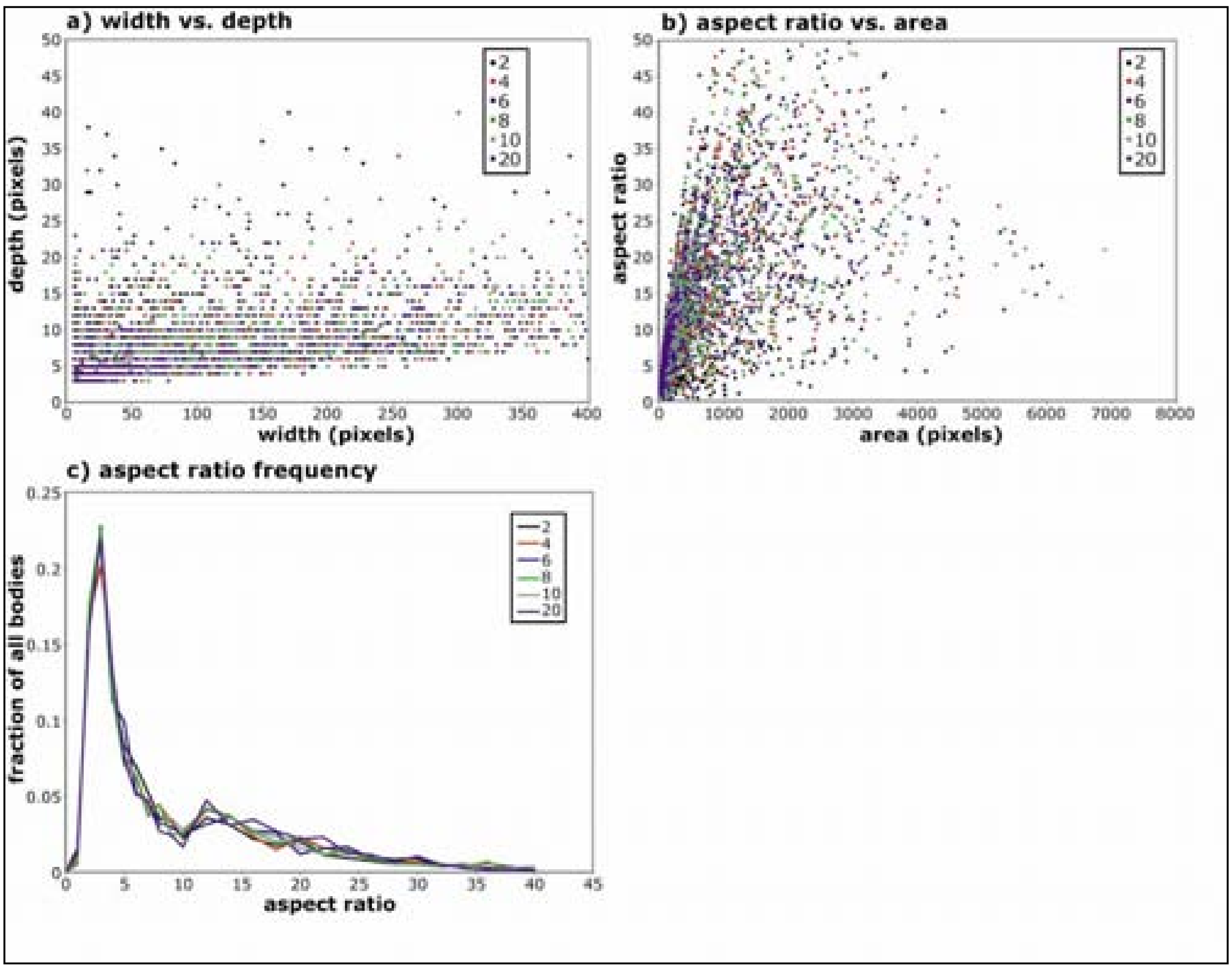

Figure 8: a) plot of depth (thickness) of depositional packages against width over various time intervals; b) plot of depositional package aspect ratio against cross-sectional area (measured in pixels); c) frequency occurrence of depositional package aspect ratios as a fraction of all packages measured over a given time interval

can cover larger widths, so may their deposits.

Figure 8c shows the frequency distribution of depositional package aspect ratio, as a proportion of all packages measured over a given time interval. Despite the apparent variability of figures 8a and b, the aspect ratios of depositional packages clearly cluster around 4—approximately the aspect ratio of the confluence scours themselves. This peak at 4, then, is the record of the channel fills. The second, though weaker, peak at an aspect ratio of 12 must be related to depositional packages produced by flow expansion downstream from confluence scours—sheet sands. This peak is more subtle, as the aspect of sheet deposits strongly depends on exactly how they intersect the topographic transect. At the proximal end of a flow expansion, the aspect ratio is relatively low, and the ratio increases with distance from the confluence scour. Therefore, depositional package aspect ratios associated with sheets, while frequently around 12, are more evenly distributed than those of channel fills.

Relationship between surface morphology and stratigraphy

The final component of our analysis of the DB 03-1 experiment to date is the actual comparison of run-time topography with stratigraphy. As the same camera and lens corrections are applied to the topographic transect images, the surface morphology images, and the stratigraphic images, all three are coincident. This allows us to superimpose topographic lines on the others, for any position along the topographic transects.

Figure 9 (images on next two pages) shows the evolution of a channel fill near the end of the experiment from initial incision through final filling. A timeline of this evolution is at the top of page 11.

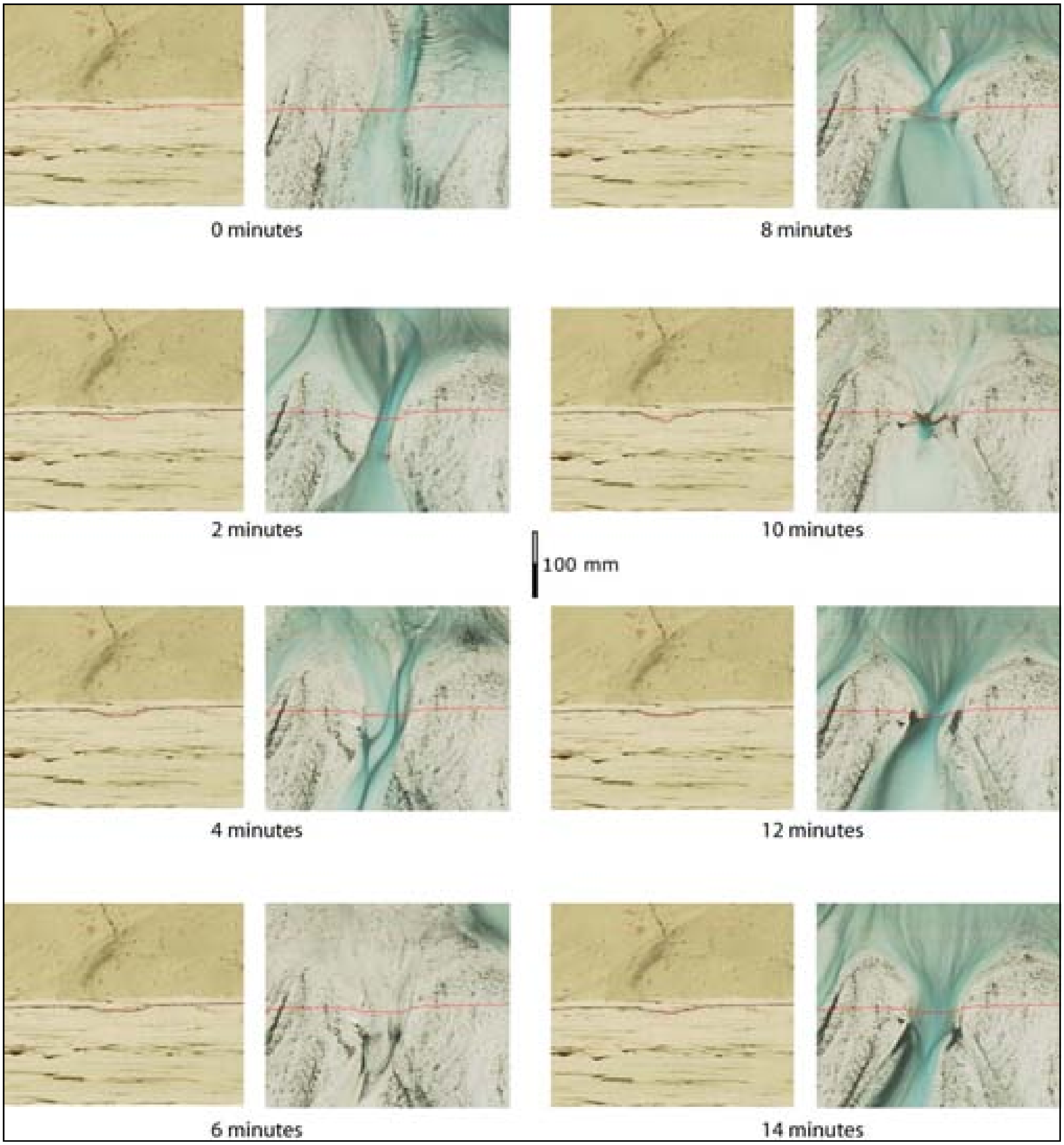

Figure 9: (this and following page) Topographic and morphological evolution from the initial cut through the final filling of a channel 2.00 m from the source. Time in this figure is relative to the first pair of images in the upper left-hand corner, which is 2 hours, 26 minutes from the end of the experiment (27 hours, 34 minutes from the start). At each time interval the surface morphology just before the topographic scan is shown (right) with that topographic scan superimposed in red. On the left is an image of the deposit showing the current topographic scan in red, and the previous (-2 minutes) in black. See text for interpretation.

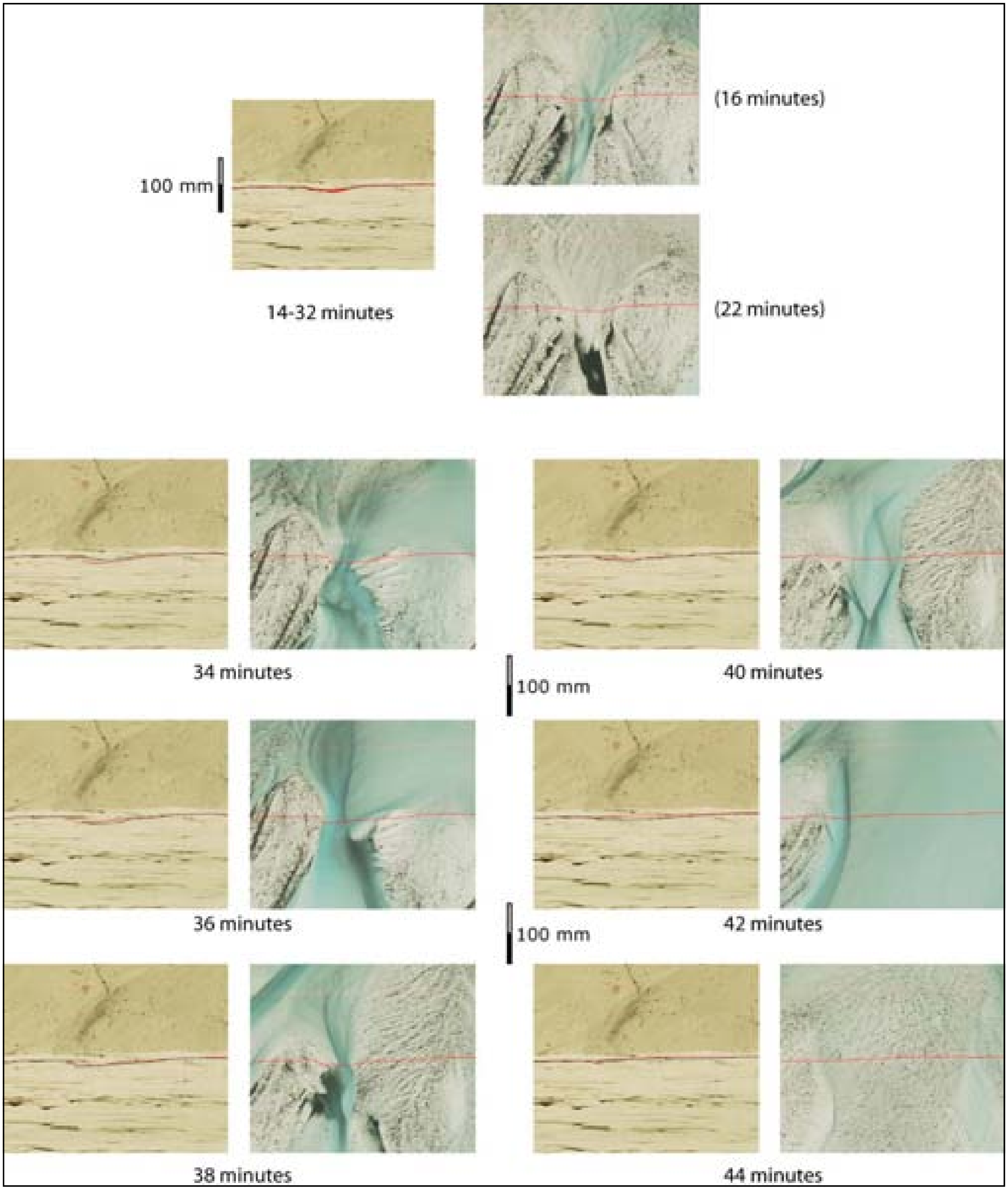
(16 minutes)
100 mm
14-32 minutes
(22 minutes)
34 minutes
100 mm
40 minutes
36 minutes
100 mm
42 minutes
38 minutes
44 minutes

Time Interval (min)	Description of Events (see figure 9 for images)
0-2:	The initial incision (approximately 10 mm) occurs over 2 minutes, as significant flow from an adjacent channel (out of the field of view up and right) is captured in a subtle pre-existing channel, converges, and scours.
2-4:	This is followed by a 2 minute interval of slight filling and widening as the flow expands locally and wanes.
4-6:	The channel actually dries up over this time-interval, as all of the flow returns to the main channel.
6-8:	Flow returns, and a new confluence and scour cuts deeper than before (to a maximum depth of ~20 mm below the initial surface at 0).
8-10:	Again, a period of widening and deposition, as the flow wanes.
10-14:	Despite apparently active flow, the topography changes little over this interval—perhaps the scour has reached some maximum efficient depth.
14-32:	The topography remains steady through this 18 minute interval, as this channel is slowly abandoned—dry by 22 minutes.
32-34:	Flow returns, this time from a slightly different breach of the main channel. This new angle of incidence produces not only a confluence scour, and erosion, but lateral migration (to the left in our perspective) at approximately 5 mm/min.
34-36:	Continued lateral migration at 5 mm/min, though no appreciable new down cutting.
36-38:	Topography indicates another episode of shallowing and widening, as much of the flow in this channel is captured by another off the left of the view. Note the appearance of coal along the left-hand channel margin
38-40:	Continued shallowing and widening
40-42:	The final filling of this channel, as a wide flow expansion from the main channel sweeps over this area. Note that the final filling, and obliteration of the channel-form topography is accomplished not by flow within this channel, but by a rapid dump of sediment by a flow from the nearby larger channel. Note, again, the presence of coal at the margin of the flow expansion. By 44 minutes this area is dry again.

Figure 10 is a detail of the channel fill structure associated with this 40-minute sequence of events. This particular sequence of events did not produce a particularly spectacular channel fill. The fill is mostly sand, though coal is deposited at the margins of the channel as it shallows and widens, as discussed in the timeline above. The final preserved fill is somewhat wider than the scours that sculpted it, though its aspect ratio is comparable to them. Despite the fact that this sequence of events occurred 3 hours from the end of the experiment, the fill was reworked by subsequent events—highlighting the dynamic nature of these systems.

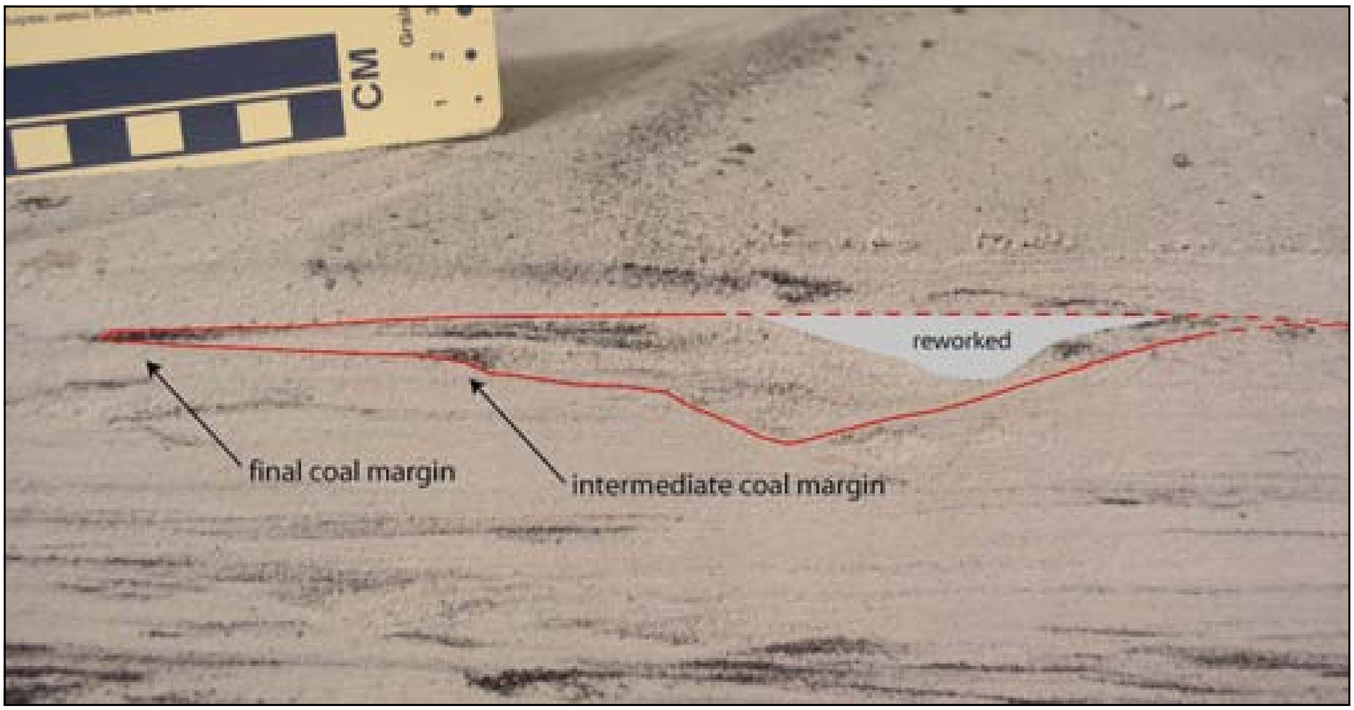

Figure 10: Detail image of channel fill associated with timeline in text and figure 9. Red line indicates approximate outline at time of deposition—dashed where removed by subsequent reworking. Annotated coal margins correspond to those indicated in intervals 36-38 and 40-42 in the timeline for figure 9.

Conclusions

1. Though the analysis is not complete, it is clear that the method for measuring topography with high temporal resolution is a success. We can watch the creation of the stratigraphic record.
2. There is poor correlation between spatially averaged aggradation rates and external forcing. Aggradation over short time intervals is a dynamic process—3 steps back for 5 steps forward—and only long-term averages of short-term behavior show hints of allocyclic behavior. That said, the external forcing in DB 03-1 was constant, and the results herein must be compared with other delta basin and Jurassic Tank data in order to qualify this statement.
3. The geometry of short-term aggradational packages reflects the fluvial processes responsible for their deposition. As a result, there is an upper limit to the aspect ratio of these packages, just as there is a physical upper limit for flow.
4. Many of the channel fill structures in these deposits represent multiple episodes of down cutting and filling. These episodes may be separated by periods of abandonment, though difficult to distinguish in the fill.

References

CAZANACLI, D. A., PAOLA, C., AND PARKER, G., 2002, Experimental steep, braided flow: application to flooding risk on fans: Journal of Hydraulic Engineering, v. 128, p. 322-330.

SHEETS, B., HICKSON, T., AND PAOLA, C., 2002, Assembling the stratigraphic record: depositional patterns and time-scales in an experimental alluvial basin: Basin Research, v. 14, p. 287-301.